INVARIANTS OF THE VELOCITY-GRADIENT TENSOR IN A SPATIALLY DEVELOPING INHOMOGENEOUS TURBULENT FLOW

Oliver R.H. Buxton

Department of Aeronautics
Imperial College London
London, SW7 2AZ, U.K.
o.buxton@imperial.ac.uk

Massimiliano Breda

Department of Aeronautics
Imperial College London
London, SW7 2AZ, U.K.
mb2014@ic.ac.uk

Xue Chen

Department of Aeronautics
Imperial College London
London, SW7 2AZ, U.K.
xue.chen11@imperial.ac.uk

ABSTRACT

Tomographic particle image velocimetry experiments were performed in the near field of the turbulent flow past a square cylinder. A triple decomposition was performed on the resulting velocity fields into a time invariant mean flow and a fluctuating velocity field, which is itself decomposed into a coherent and a residual/stochastic fluctuating velocity field. The statistical distributions of the second and third invariants of the velocity-gradient tensor were then computed at various streamwise locations, along the centre line of the flow and within the shear layers. These invariants were calculated from "classical" Reynolds-decomposed fluctuating velocity fields in addition to the coherent and stochastic fluctuating velocity fields. The range of spatial locations probed incorporates regions of contrasting flow physics, including a mean recirculation region and separated shear layers, both upstream and downstream of the location of peak turbulence intensity along the centre line. These different flow physics are also reflected in the velocity gradients themselves with different topologies, as characterised by the statistical distributions of the constituent enstrophy and strain-rate invariants, for the three different fluctuating velocity fields. Despite these differing flow physics the ubiquitous self-similar "tear drop"-shaped joint probability density function between the second and third invariants of the velocity-gradient tensor is observed along the centre line and shear layer when calculated from both the Reynolds decomposed and the stochastic velocity fluctuations. These "tear drop"-shaped joint probability density functions are not, however, observed when calculated from the coherent velocity fluctuations. This "tear drop" shape is classically associated with the statistical distribution of the velocity-gradient tensor invariants in fully developed turbulent flows in which there is no coherent dynamics present, and hence spectral peaks at low wavenumbers. The results presented in this paper, however, show that such "tear drops" also exist in spatially developing inhomogeneous turbulent flows.

INTRODUCTION

The general topology of the fine scales of turbulence may be shown to depend on the invariants of the velocity-gradient tensor, VGT henceforth. The VGT may be split up into a symmetric and skew-symmetric component, the strain-rate and rotation tensors respectively,

$$a_{ij} = \frac{\partial u_i'}{\partial x_j} = s_{ij} + \omega_{ij} = \frac{1}{2}\left(\frac{\partial u_i'}{\partial x_j} + \frac{\partial u_j'}{\partial x_i}\right) + \frac{1}{2}\left(\frac{\partial u_i'}{\partial x_j} - \frac{\partial u_j'}{\partial x_i}\right) \quad (1)$$

in which u_i' denotes the fluctuating components of velocity from a classical Reynolds decomposition. These invariants are the coefficients in the characteristic equation for the VGT of the form

$$\xi^3 + P\xi^2 + Q\xi + R = 0. \quad (2)$$

For an incompressible flow $P = a_{ii} = 0$, hence the generalised topology of the flow may be described by Q and R, defined as

$$Q = \frac{1}{4}\left(\omega_i\omega_i - 2s_{ij}s_{ij}\right) = Q_\omega + Q_S \quad (3)$$

$$R = -\frac{1}{3}\left(s_{ij}s_{jk}s_{ki} + \frac{3}{4}\omega_i s_{ij}\omega_j\right). \quad (4)$$

The joint probability density function (pdf) between Q and R, $f(Q,R)$, is observed to make self-similar "tear drop" shapes in a variety of fully developed turbulent flows leading to it being described as a "universal" feature of small-scale turbulent motions (Elsinga & Marusic, 2010).

The vast majority of studies examining $f(Q,R)$ have done so in fully developed turbulent flows, in which the spectrum of turbulent kinetic energy is akin to the model spectrum proposed by Pope (2000). More recently, however, Gomes-Fernandes *et al.* (2014) have examined the evolution of the state of the VGT in a spatially developing turbulent flow generated by a multi-scale space-filling fractal square grid. For such an inhomogeneous flow it was observed that the "tear drop" shape of the joint pdf gradually unfolds with distance x travelled downstream.

A characteristic of many spatially developing inhomogeneous turbulent flows is that they contain a significant energy content in coherent dynamics due to, for example, vortex shedding in bluff body flows or Kelvin-Helmholtz instabilities in shear layers. Crucially, these coherent dynamics are a consequence of large-scale

instabilities within the flow that will scale with the largest relevant/global length scales. It is thus not reasonable to consider them statistically homogeneous or isotropic, as are the fine scales of turbulence. The presence of such coherent dynamics led to the introduction of a triple decomposition of the form

$$U_i = \overline{u}_i + \underbrace{u_i^{\phi} + u_i''}_{u_i'} \tag{5}$$

in which $\overline{u}_i$ is the (time-averaged) base flow and the fluctuating component of the classical Reynolds decomposition, u_i', is further decomposed into a coherent fluctuation u_i^{ϕ} and a stochastic fluctuation u_i'' (Hussain & Reynolds, 1970).

This paper will thus examine the spatial evolution of the invariants of the VGTs, $a_{ij} = \partial u_i'/\partial x_j$, $a_{ij}^{\phi} = \partial u_i^{\phi}/\partial x_j$ and $a_{ij}'' = \partial u_i''/x_j$. The particular flow chosen is that past a high aspect ratio (effectively infinitely long) square cylinder, at a sufficiently high Reynolds number to ensure that the flow is adequately turbulent.

METHODOLOGIES AND POST PROCESSING

The experiments, fully documented in Buxton *et al.* (2017), were performed in a water tunnel which has a cross section of 600×600 mm^2. A high aspect ratio ($AR = 16$) square cylinder of side length $D = 32$ mm was mounted just downstream of the contraction of the tunnel perpendicularly to the incoming flow. This configuration yielded a Reynolds number based on the cylinder side length and free-stream velocity of $Re_D = 10,840$. Throughout this paper a Cartesian coordinate system, $x-y-z$ (streamwise - cross-stream - spanwise) with corresponding velocity components $U-V-W$, is adopted with an origin located on the centre of the rear face of the cylinder.

Tomographic PIV experiments were conducted that imaged the flow immediately downstream of the cylinder in a field of view (FOV) that measured $3.8D \times 2D \times 0.168D$ with $N = 2,000$ ($\times 4$ cameras) image pairs being captured. This spatial resolution equates to approximately 11η, where η is the Kolmogorov length-scale, for $x/D \gtrsim 1.5$ up to a worst case scenario of $\approx 17\eta$ in the separated shear layers at $x/D = 0$. Whilst a spatial resolution of $\approx 3\eta$ is generally considered necessary to resolve the smallest, dissipative length scales within a turbulent flow it has been shown that resolving the characteristic "tear-drop" shape of the joint pdf between Q and R is reliant upon a mix of dissipative and inertial range scales $> \lambda$, where λ is the Taylor micro-scale (Buxton, 2015). The spatial resolution of the present data easily meet this criteria (it is no worse than 0.4λ and remains better than 0.15λ everywhere other than within the mean recirculation region) and thus this data set may be considered adequately spatially resolved to examine $f(Q,R)$. The resultant velocity fields were differentiated in space using an in-house fourth order accurate finite differences approximation. In order to correct for any non-zero divergence due to intrinsic experimental noise the data were post-processed using the divergence correction scheme of de Silva *et al.* (2013).

The triple decomposition of (5) was carried out by phase averaging the fluctuations u_i', calculated by subtraction from the time average $\overline{u}_i$, into 18 phase bins of extent $\phi_m \pm 10^{\circ}$. Proper orthogonal decomposition (POD) was performed in order to obtain the phase angle of each instantaneous velocity field. Perrin *et al.* (2007) (amongst others) shows that the first two POD modes correspond to the vortex shedding in the flow past a cylinder. The phase angle of an instantaneous velocity field was computed from the time-varying mode coefficients, a_1 and a_2 of these two POD modes. Finally, the stochastic velocity fluctuation is the residual of $(U_i - \overline{u}_i - u_i^{\phi})$. Computation of the overall turbulent kinetic energy showed that this decomposition was energy preserving due to the observation that the correlation $\langle u_i^{\phi} u_i'' \rangle \approx 0$.

RESULTS AND DISCUSSION

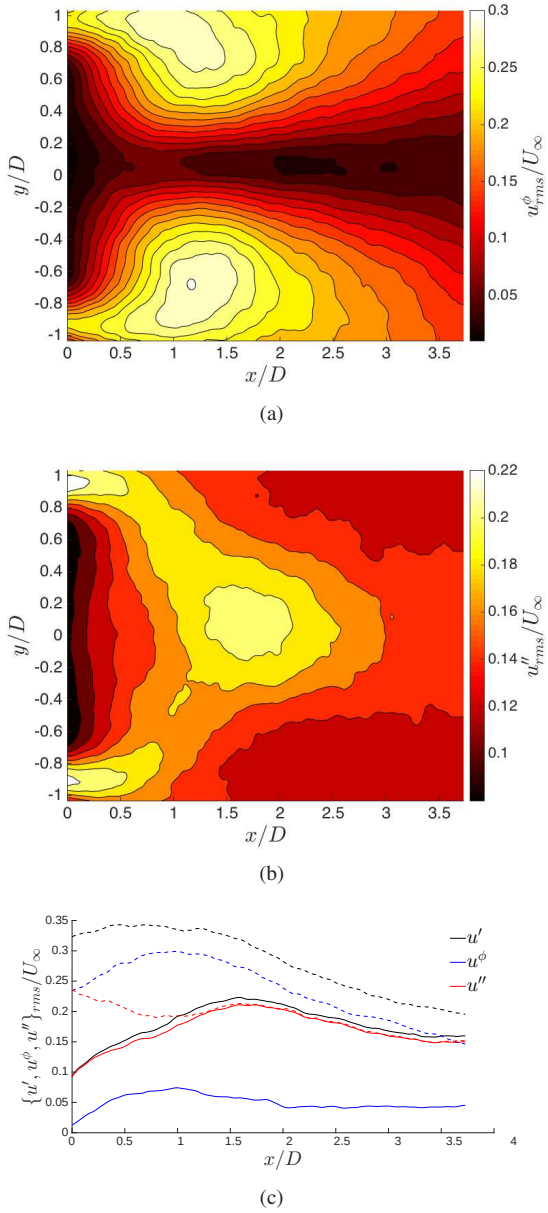

Figure 1. R.m.s. fields of the coherent (a) and stochastic (b) component of the streamwise velocity fluctuation. (c) streamwise profiles of r.m.s. of $\{u', u^{\phi}, u''\}$ along the centre-line (solid lines) and along the shear layers (dashed lines), defined as the locations, $y(x)$, at which the r.m.s. is locally a maximum.

The various fluctuating velocity fields, $\boldsymbol{u}'(\boldsymbol{x})$, $\boldsymbol{u}^{\phi}(\boldsymbol{x})$ and $\boldsymbol{u}''(\boldsymbol{x})$ which are illustrated in figure 1, were differentiated spatially according to the fourth order-accurate scheme described previously and the various invariants of the velocity-gradient tensor were computed. The spatial evolution of the joint pdfs of these invariants was computed along two streamwise traverses, the centre line of the flow ($y = 0$) and along the shear layers. At a given x location

the y profiles of the r.m.s. of u' have two local maxima, and thus the shear layers were defined as the locations, $y(x)$, of these maxima. Due to the typically observed intermittent distribution of the velocity gradients some spatial averaging was performed, in which a square window of size $0.13D \times 0.13D$ was centred on the point of interest (i.e. on the centre line or the shear layer) in order to better converge the statistics. A sensitivity study was conducted to assess the size of this window on the ability to faithfully re-produce the $Q-R$ joint pdf and it was found to be optimal in the sense that it was the minimal window size that generated relatively noise-free statistics that were insensitive to modest changes in window size.

Joint pdfs were then produced of the various $Q-R$ invariants, computed from the $\{a_{ij}, a_{ij}^{\phi}, a_{ij}''\}$ fields, at various streamwise locations. In order to make a direct comparison between the joint pdfs computed from the various fields of velocity gradients we wished to choose a contour level that encompasses an equivalent proportion of the overall data available, i.e.

$$\iint_A f_{QR}(Q,R)\mathrm{d}R\mathrm{d}Q = \Sigma = \text{const.} \tag{6}$$

The choice of Σ is arbitrary, but we wished to choose a contour level defining A that was sufficiently rare to ensure that we captured a broad range of Q,R states but sufficiently common to ensure a reasonably smooth contour from sufficiently converged statistics. We chose a contour level such that $\Sigma = 0.683$, which is equivalent to the proportion of data bounded by $\pm\sigma$ (one standard deviation) for a univariate Gaussian distribution. The invariants themselves are all normalised by the local value of $\langle Q_\omega \rangle$, computed from the relevant velocity-gradient field such that the joint pdfs of figure 2(c), for example, are normalised by $\langle Q_\omega \rangle$ calculated from the a_{ij}^{ϕ} field at the centre line and appropriate x-location etc.

It can be seen that the classical "tear drop" shape for the joint pdf is recovered when calculated from the a_{ij} field. This in itself is a surprising result since the "tear drop" shape of the $Q-R$ joint pdf is considered to be associated with fully developed turbulent flows. Although there is no clear definition of such a flow they may be generally considered to be close to homogeneous and isotropic (requiring the integral length scale to be smaller than a relevant homogeneity length scale), in the small scales at least, with mean velocity profiles that may be collapsed when scaled by a relevant flow variable such as the centre line velocity for a wake. Evidently these criteria are far from being met in the near-field flow behind a square cylinder. Further, the "tear drop"-shaped contours are equally visible, and quantitatively similar (with the exception of the $x/D = 3.5$ cases) on both the centre line and the shear layers in figures 2(a) and (b). This is despite the fact that the flow physics for both of these regions differ significantly. Along the centre line the shape of the $Q-R$ joint pdf contours are similar regardless of whether the data are extracted from the mean circulation region (for the centre line) or downstream of this in the turbulence decay region ($x/D = 2$). Perversely, $x/D = 3.5$ is perhaps the location where one might assume that the criteria for a fully developed turbulent flow, for which the "tear drop"-shaped joint pdf is considered to be a universal feature, are more stringently met than any of the streamwise locations further upstream. Despite this, the joint pdfs from this location are the only ones not to collapse when normalised by $\langle Q_\omega \rangle$. The clearly defined "tear drop"-shaped contours of the joint pdfs of figures 2(a) and (b) are in contrast to the spatially developing fractal square grid flow of Gomes-Fernandes *et al.* (2014), in which the "tear drop" shape was observed to unfold as the flow develops downstream.

Comparison of figures 2(a) and (b) shows that the collapse of the contours of $f_{QR}(Q,R)$ when scaled with the local quantity $\langle Q_\omega \rangle$ is marginally better along the shear layer than the centre-line, excluding the data from $x/D = 3.5$. There is significant energy content in coherent motions in the shear layers, as illustrated in figure 1(a), whereas along the centre-line there is virtually none with a significant contribution to the total turbulent kinetic energy from the u_i'' fluctuations. It is thus a surprising result that the collapse of the contours of $f_{QR}(Q,R)$ is better where there is a significant contribution from coherent motions as opposed to primarily the stochastic fluctuations. Nevertheless, the similarity between the contours of figure 2(a) and (b) is stark, despite the fact that they are computed from regions with very different flow physics to one another. The streamwise location at which the joint pdf most resembles that for fully developed turbulence, with an enhanced contribution from sector I (defined in figure 2(a)) and elongated "Vieillefosse tail" is at the location of peak turbulence intensity, $x/D = 1.104$.

Figures 2(c) and (d) show the equivalent joint pdfs between Q and R computed from the coherent velocity-gradient field, a_{ij}^{ϕ}, along the centre line and shear layer respectively whilst (e) and (f) show those computed from the stochastic velocity-gradient field, a_{ij}''. It is clear that the contours of $f_{QR}(Q,R)$ computed from the a_{ij}^{ϕ} field do not exhibit anything remotely akin to a "tear drop" shape, whilst those computed from the a_{ij}'' field do, and are indeed quantitatively very similar to those computed from the a_{ij} field. If anything, it may be commented that the contours show a better collapse with the local $\langle Q_\omega \rangle$ scaling for the joint pdf computed from the a_{ij}'' field than from the a_{ij} field. Again, however, the notable exception is the contour extracted from the data at the furthest downstream location, $x/D = 3.5$, at which we may have expected the flow to best approximate a "fully developed flow".

We may thus conclude from figure 2 that in this spatially developing inhomogeneous flow the "tear drop" shape of the contours of the joint pdf between Q and R is almost entirely due to the stochastic turbulent fluctuations. Even though $\langle Q_\omega^{\phi} \rangle$ is non-negligible, indicative of the average magnitude of the a_{ij}^{ϕ} tensor, it does not contribute to the kinematics of the overall velocity-gradient tensor through the Q - R joint pdf. It thus appears that the "tear drop" is more ubiquitous than first thought since it appears in flows with significantly varied physics, for example fully developed/spatially developing/recirculation/separated shear layers etc. Further, the statistical behaviour of the invariants of the VGT does not vary significantly in space along either the centre line or the shear layer despite the rapidly changing flow physics. To quantitatively illustrate the spatially developing nature of the flow physics, specific to the VGT itself, figure 3 presents the joint pdfs of the constituent components of the invariant Q; Q_ω is the first term on the right hand side of (3) and Q_S is the second term on the right hand side of (3). The various joint pdfs are again normalised by the local (and field-specific) values of $\langle Q_\omega \rangle$ and the data are extracted along the centre line and shear layers at the same x locations as with the joint pdfs of figure 2. All contour lines presented again encompass 68.3% of the total available data within the $0.13D \times 0.13D$ interrogation windows from which the statistics are computed.

The topology of the fine-scale turbulent motions can be inferred from such joint pdfs. The $-Q_S \sim s_{ij}s_{ij}$ axis represents points with a locally high rate of dissipation of turbulent kinetic energy which are known to be arranged in sheet-like structures (e.g. Ganapathisubramani *et al.*, 2008) whereas the $Q_\omega \sim \omega_i\omega_i$ axis is associated to points with a locally high enstrophy which are arranged in tube-like structures in turbulent flows (e.g. Jiménez *et al.*, 1993). The 45° line of $-Q_S = Q_\omega$ represents a balance of enstrophy and dissipation and these points may be somewhat vaguely described as vortex sheets. Nevertheless, it has been shown that a very large proportion of the data for fully developed turbulent mixing layers lies along this line (Soria *et al.*, 1994). Indeed of all the contours of figures 3(e) and (f) those extracted from the location of peak tur-

bulence intensity, $x/D = 1.104$ (the red contours), look the most similar to those computed from fully developed turbulence. Despite the similarity of the flow topology for all of the VGT fields, as illustrated in figure 3, the joint pdfs of figures 2(c) and (d) are vastly different to the classical "tear drop" shape for the joint pdf between Q and R.

A particularly clear preference for high enstrophy, tube-like, topology exists in the downstream locations of the a_{ij}^{ϕ} field, both along the shear layers and the centre line (where admittedly the energy content of $\boldsymbol{u}^{\phi}(\boldsymbol{x})$ is low). This tendency develops with x since the topology of a_{ij}^{ϕ} shows a tendency for vortex sheets further upstream. In this instance the very different flow physics/topologies at the various downstream locations presented in figure 3(d) do translate into quantitatively different joint pdfs between Q and R in figure 2(d), which are far from "tear drop"-shaped. Contrastingly, it may be observed that (with the exception of $x/D = 3.5$) the joint pdfs between Q and R computed from the a_{ij} field, figures 2(a) and (b), collapse onto self-similar "tear drop" shapes despite the fact that no such collapse is observed in the joint pdfs between Q_ω and $-Q_S$ in figures 3(a) and (b). This is true along the centre line of the flow, in which there is initially a recirculation region before spatially developing into a turbulent wake flow, as well as along the shear layers. Along the shear layers there is a clear preference for high enstrophy structures to develop with increasing x, whereas along the centre line there are very different distributions as the flow transitions from a mean re-circulation to a vortex street. Nevertheless, all of these regions produce "tear drop"-shaped joint pdfs between Q and R.

CONCLUSIONS

Tomographic PIV experiments were performed in the near-field of the turbulent flow around a square cylinder generating a three-dimensional three component (3D3C) data set. The velocity field was decomposed, according to (5), into a time invariant base flow, a coherent fluctuation and a residual/stochastic fluctuation. This was conducted by means of phase bin-averaging in which the phase angle of each instantaneously acquired 3D3C velocity field was calculated from the time-varying mode coefficients of the first and second modes obtained from a proper orthogonal decomposition of the flow field. These two modes correspond to the vortex shedding downstream of the cylinder. From these three separate velocity fields the invariants of the velocity-gradient tensor were computed and their statistics compared to one another. Since the flow is spatially developing and inhomogeneous these statistics were computed both upstream, including from within the mean recirculation region, and downstream of the location of peak turbulence intensity along the centre line of the flow. Additionally, the statistics were extracted from the shear layer region of the flow; so-defined as the local maximum in turbulence intensity at a given downstream location, x.

Joint pdfs between the rotating and straining constituents of the invariant Q, Q_ω and Q_S respectively, highlighted the very different flow physics and topologies of the various velocity-gradient fields at the various spatial interrogation locations. Despite the differing flow physics and topologies of the various fields of velocity gradients the joint pdfs between the second and third invariants, Q and R, resembled the classical "tear drop" shapes associated with fully developed turbulence when computed from the total and stochastic velocity gradients. In fact the contours of the joint pdfs were found to collapse in a self-similar fashion when appropriately normalised by the local ensemble average of Q_ω. Such self-similar "tear drop" shapes were found along the centre line and the shear layer at all but the farthest downstream locations. Observation of the relative contributions of the rotationally dominated sectors I and II showed that these tended to be in balance with one another and only very slowly variant in space, although their values did change according to which velocity-gradient field they were computed from. The statistics of the inviscid source/sink terms in the evolution of the enstrophy and dissipation were also observed to collapse remarkably well with the local value of $\langle Q_\omega \rangle$ (not shown for brevity), offering a potential explanation for the collapse of the "tear drop"-shaped joint pdfs. As expected the joint pdfs computed from the coherent velocity gradients did not resemble those from fully developed turbulence.

It thus seems that the ubiquitous "tear drop"-shaped statistical distribution of the invariants of the velocity-gradient tensor is even more ubiquitous than first thought. Not only does it appear in a manner of (homogeneous) fully developed turbulent flows, but this manuscript also shows that it exists in inhomogeneous flows with rapidly spatially varying flow physics. Whilst fully developed flows have a flat spectrum of turbulent kinetic energy at the low wavenumbers the flow past a square cylinder has a clear spike at the vortex shedding wavenumber. From this perspective we should thus consider the "tear drop"-shaped joint pdf between the invariants of the velocity-gradient tensor not as a universal feature of fully developed turbulence (Chacin & Cantwell, 2000; Elsinga & Marusic, 2010) but as a universal feature of turbulent flows.

REFERENCES

Buxton, O.R.H. 2015 Modulation of the velocity gradient tensor by concurrent large-scale velocity fluctuations in a turbulent mixing layer. *Journal of Fluid Mechanics* **777**, R1:1–12.

Buxton, O.R.H., Breda, M. & Chen, X. 2017 Invariants of the velocity-gradient tensor in a spatially developing inhomogeneous turbulent flow. *Journal of Fluid Mechanics* **817**, 1–20.

Chacin, J.M. & Cantwell, B.J. 2000 Dynamics of a low Reynolds number turbulent boundary layer. *Journal of Fluid Mechanics* **404**, 87–115.

Elsinga, G.E. & Marusic, I. 2010 Universal aspects of small-scale motions in turbulence. *Journal of Fluid Mechanics* **662**, 514–539.

Ganapathisubramani, B., Lakshminarasimhan, K. & Clemens, N.T. 2008 Investigation of three-dimensional structure of fine-scales in a turbulent jet by using cinematographic stereoscopic PIV. *Journal of Fluid Mechanics* **598**, 141–175.

Gomes-Fernandes, R., Ganapathisubramani, B. & Vassilicos, J.C. 2014 Evolution of the velocity-gradient tensor in a spatially developing turbulent flow. *Journal of Fluid Mechanics* **756**, 252–292.

Hussain, A. K. M. F. & Reynolds, W. C. 1970 The mechanics of an organized wave in turbulent shear flow. *Journal of Fluid Mechanics* **41**, 241–258.

Jiménez, J., Wray, A.A., Saffman, P.G. & Rogallo, R.S. 1993 The structure of intense vorticity in isotropic turbulence. *Journal of Fluid Mechanics* **255**, 65–90.

Perrin, R., Braza, M., Cid, E., Cazin, S., Barthet, A., Sevrain, A., Mockett, C. & Thiele, F. 2007 Obtaining phase averaged turbulence properties in the near wake of a circular cylinder at high Reynolds number using POD. *Experiments in Fluids* **43** (2), 341–355.

Pope, S.B. 2000 *Turbulent Flows*. Cambridge University Press.

de Silva, Charitha M., Philip, Jimmy & Marusic, Ivan 2013 Minimization of divergence error in volumetric velocity measurements and implications for turbulence statistics. *Experiments in Fluids* **54** (7), 1–17.

Soria, J., Sondergaard, R., Cantwell, B. J., Chong, M. S. & Perry, A. E. 1994 A study of the fine-scale motions of incompressible time-developing mixing layers. *Physics of Fluids* **6** (2), 871–884.

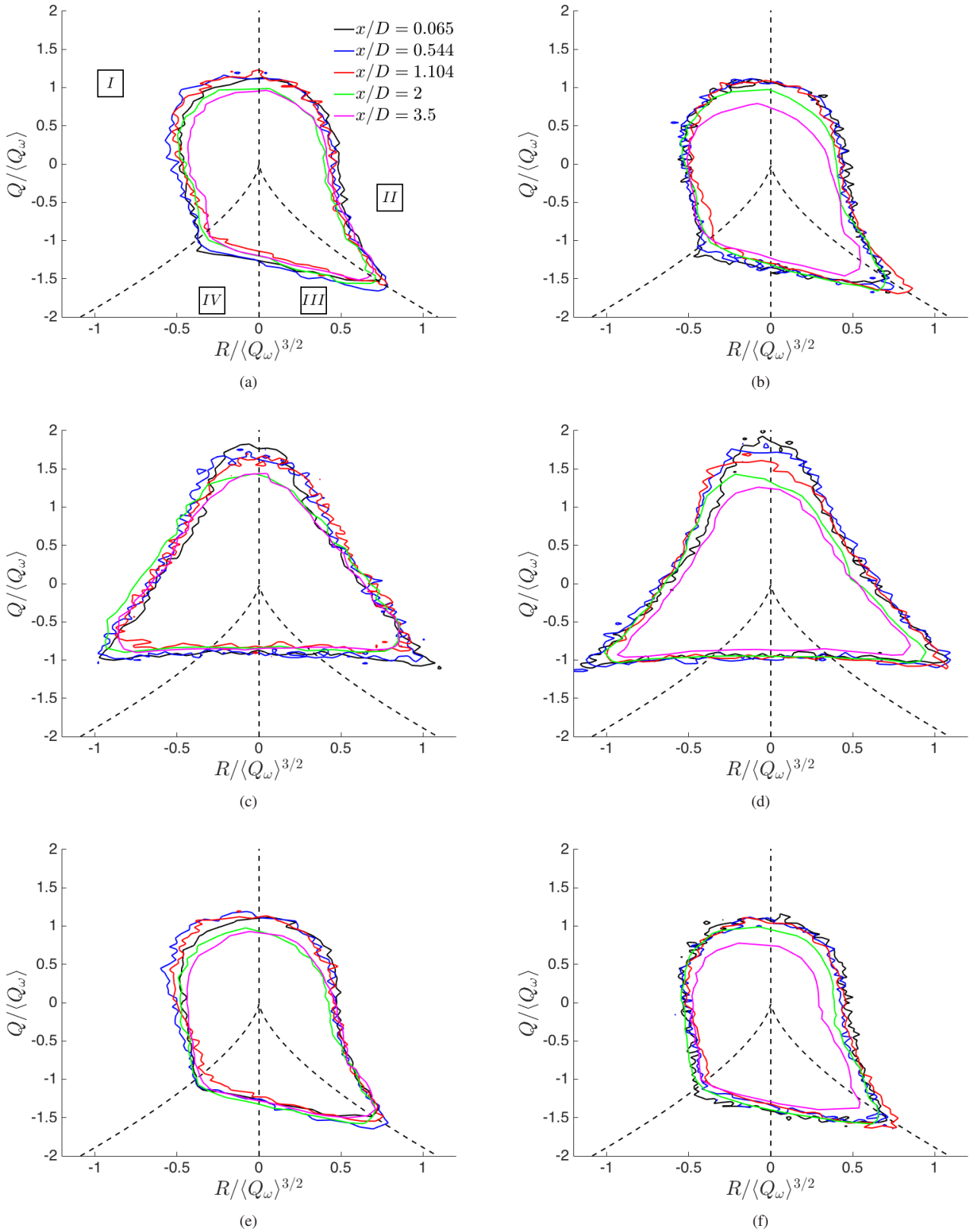

Figure 2. Joint pdfs between Q and R along the centre line (left hand column) and the shear layer (right hand column) for the a_{ij} (first row), a^{ϕ}_{ij} (middle row) and a''_{ij} (bottom row) velocity-gradient fields. The dashed lines denote $R = 0$ and $\Delta = Q^3 + (27/4)R^2 = 0$, where Δ is the discriminant of (2) separating swirling ($\Delta > 0$) and straining ($\Delta < 0$) solutions. These lines allow the $Q-R$ space to be partitioned into four sectors ($I-IV$) according to the dominant flow physics.

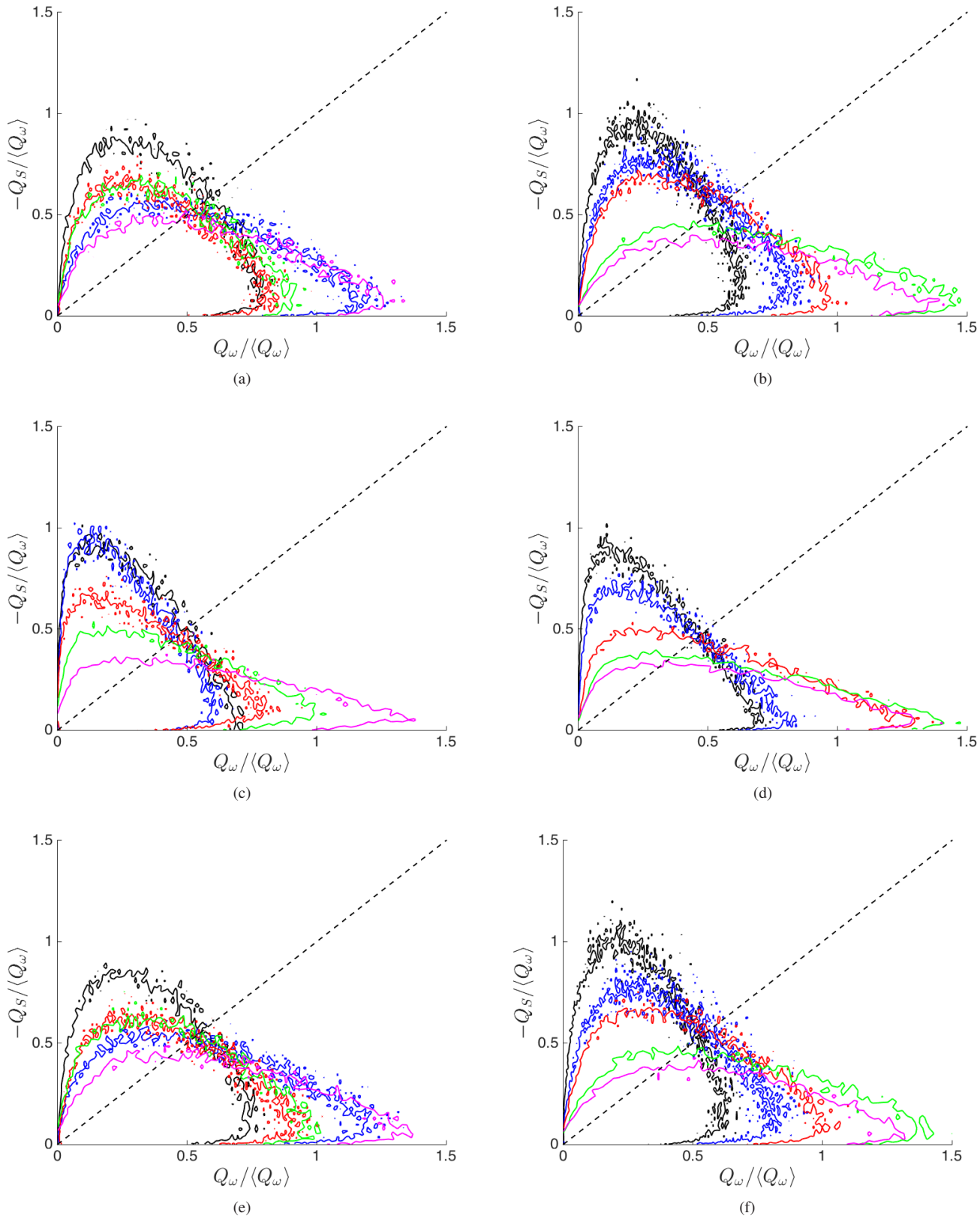

Figure 3. Joint pdfs between Q_ω and $-Q_S$ along the centre line (left hand column) and the shear layer (right hand column) for the a_{ij} (first row), a_{ij}^{ϕ} (middle row) and a_{ij}'' (bottom row) velocity-gradient fields. The dashed line denotes $-Q_S = Q_\omega$. The contour colours correspond to the equivalent streamwise locations as those identified in figure 2.